A Robust Position/Force Learning Controller of Manipulators via Nonlinear $H\infty$ Control and Neural Networks

Ming-Chang Hwang and Xiheng Hu

***Abstract*—A new robust learning controller for simultaneous position and force control of uncertain constrained manipulators is presented. Using models of the manipulator dynamics and environmental constraint, a task-space reduced-order position dynamics and an algebraic description for the interacting force between the manipulator and its environment are constructed. Based on this treatment, the robust nonlinear $H\infty$ control approach and direct adaptive neural network (NN) technique are then integrated together. The role of NN devices is to adaptively learn those manipulators' structured/unstructured uncertain dynamics as well as the uncertainties with environmental modelling. Then, the effects on tracking performance attributable to the approximation errors of NN devices are attenuated to a prescribed level by the embedded nonlinear $H\infty$ control. Whenever the adopted NN devices have the potential to effectively approximate those nonlinear mappings which are to be learned, then this new control scheme can be ultimately less conservative than its counterpart $H\infty$ only position/force tracking control scheme. This is shown analytically in the form of theorem. Finally, a simulation study for a constrained two-link planar manipulator is given. Simulation results indicate that the proposed adaptive $H\infty$ NN position/force tracking controller performs better in both force and position tracking tasks than its counterpart $H\infty$ only position/force tracking control scheme.**

***Index Terms*—Adaptive neural networks, H_∞, simultaneous position/force control.**

I. Introduction

OVER the past few years, the approach of applying nonlinear $H\infty$ control to the motion control problem of robotic manipulators has received considerable attention [1]–[4]. A convenient point of this approach is that it can attenuate the effects of various uncertainties (e.g., structured parametric uncertainty and unstructured disturbance) on tracking performance to a required level without the assumption that those uncertain parameters and disturbances belong to a known compact set. Therefore, the nonlinear $H\infty$ control approach does not require the nontrivial effort of estimating the bounding functions of uncertainties, which is usually required in the other nonlinear robust control schemes, e.g., sliding mode and saturating-type control schemes.

It is worth noting that motion controllers do not explicitly take account of those forces acting on their end-effectors. Therefore, motion controllers are more suitable for manipulators operating in "free space," e.g., robotic applications for spray painting and inspection. However, many robotic applications require their end-effectors to be in contact with an environment, e.g., robotic applications for grinding, assembly, deburring, etc. In such a robotic application, not only will the motion of the end-effector be required to follow a prescribed path, but also the force exerted by the end-effector on its environment will be required to track a pre-defined trajectory. In other words, those forces generated between the end-effector and its environment should be accommodated instead of being treated as disturbances and being rejected. Therefore, those well-developed nonlinear $H\infty$ controllers for motion control problems cannot be directly employed in the simultaneous position/force tracking control problem.

Many approaches have been proposed for this simultaneous position/force tracking control problem; the well-organized survey papers [5]–[8] have summarized a vast number of control schemes for this control problem. Interested readers are suggested to have a look at these survey papers and the references cited therein. One of the best known approaches in these literatures is the so-called hybrid control [9]. The underlying concept of hybrid control is to identify and decouple the degrees of freedom of position-controlled subspace from those of force-controlled subspace, such that position and force information can be analyzed independently to take advantage of well-developed linear/nonlinear control techniques. Then, at the final control design stage, the position sub-controller and the force sub-controller are combined together.

Through the concept of hybrid control, the so-called reduced-order force control method was pioneered by McClamroch and Wang [10]. In [10], a nonlinear coordinate transformation was constructed to produce a joint-space reduced-order dynamic model which explicitly incorporated the constraint description and force. Using this model, a modified computed torque control architecture was then developed that decoupled the position- and force-controlled degrees of freedom without requiring orthogonality as a necessary condition. Through the treatments in [10], the hybrid position/force control concept was then for the first time theoretically justified. A task-space reduced-order force control method was proposed in [5]. This method used a coordinate transformation that generalized the methods of decoupling force effects from position dynamics and that had as special cases several other

Manuscript received October 7, 1998; revised January 5, 2000. This paper was recommended by Associate Editor R. A. Hess.

The authors are with the School of Information and Electrical Engineering, The University of Sydney, NSW 2006, Australia (e-mail: hwang@ee.usyd.edu.au).

Publisher Item Identifier S 1083-4419(00)02969-1.

reduced-order force control methods, including the method in [10]. This task-space reduced-order force control method assumed exact knowledge about environmental constraints.

On the other hand, exploiting the function approximation capacity of neural networks (NN's) for the simultaneous position/force control problem has also attracted attention [11]–[16]. Reference [12] used NN to compensate for various uncertainties through the learning by repetition of the working task. References [13] and [14] utilized NN within the impedance force-control framework. Reference [15] used NN within the hybrid control framework of [9]. The NN devices in this control scheme required an off-line training phase. Reference [16] employed NN with a joint-space reduced-order model. This control scheme required an explicit construction of bounding function.

From the review of previous literature, it is also believed that a control scheme integrating the direct adaptive NN technique with a nonlinear $H\infty$ control for this simultaneous position/force control problem within the reduced-order force control framework has not yet been reported. To contribute toward the identified gaps in the control literature of constrained manipulators, a new simultaneous position/force tracking control scheme is proposed here. In the proposed control scheme, the parametric uncertainties and disturbances in manipulator dynamics as well as the geometry and stiffness uncertainties in environmental modelling will all be taken into account. In this control scheme, based on a model of task-space reduced-order position dynamic and an algebraic model of interacting forces between the end-effector and its environment, the learning capability of NN devices is then implanted into a nonlinear $H\infty$ control design. Firstly, the function approximation capacity of NN devices is exploited for adaptively learning the structured/unstructured uncertain dynamics in the manipulator model as well as the geometry and stiffness uncertainties in the environmental modelling. Secondly, the effects on tracking performance of the approximation errors of the NN devices are then attenuated to a prescribed level by the embedded nonlinear $H\infty$ controller. Because the whole control scheme can begin with a $H\infty$ tracking performance being satisfied, the NN devices do not require any off-line training phase. Also, since the NN structure can be the same regardless of the kind of manipulator, tedious and nontrivial dynamical analyses for determining a regressor, as in a conventional adaptive control scheme, are not required. Whenever the adopted NN devices have the potential to effectively approximate those nonlinear mappings which are to be learned, this control scheme can ultimately have a smaller upper bound on the $H\infty$ performance index than its counterpart suboptimal $H\infty$ only position/force tracking control scheme. This will be analytically shown in Theorem 3. Finally, a simulation study for a constrained two-link planar manipulator is given to demonstrate the priority and applicability of the proposed adaptive $H\infty$ NN position/force tracking controller.

This paper is organised as follows: In Section II, the dynamics of rigid manipulators are first reviewed, and the adopted assumptions on environmental constraints are also given. Then. the required reduced order position dynamics and the algebraic force model are derived. Section III reviews the operating mechanism of a multilayered feedforward NN structure and gives the required auxiliary analyses for applying the function approximation capacity of this NN structure. In Section IV, the definition of $H\infty$ tracking performance and the adaptive $H\infty$ NN position/force tracking control scheme are given, and the properties associated with this control scheme are discussed. The correlated suboptimal $H\infty$ only position/force tracking control scheme is also presented in Section V. Then, the fact that the conservatism in this $H\infty$ only control scheme can be further reduced by the adaptive learning of a suitably constructed NN is formally proved in Theorem 3. In Section VI, a simulation comparison between these two $H\infty$ based position/force tracking control schemes for a constrained two-link planar manipulator is given. Finally, Section VII concludes.

Notation. $\|\cdot\|$ denotes the Euclidean norm, namely, $\|x\| = \sqrt{x^T x}$, and $\|x\|_Q$ denotes $\sqrt{x^T Q x}$, where $Q = Q^T > 0$. We say that $x(\cdot) \in L_{2e}$, the extended L_2 space, if $\int_0^T \|x(t)\|^2\, dt \leq \infty$, for all finite $T \geq 0$.

II. System Modelling

A. Manipulator Dynamics

The overall plant considered in this paper consists of two subsystems: a mechanical subsystem which represents the dynamics of an n-link, revolute, serial-connected, rigid arm and an environmental constraint. After application of the well-known Lagrangian formulation [17], the mechanical subsystem can be described as

$$M_l(q_l)\ddot{q}_l + C(q_l, \dot{q}_l)\dot{q}_l + G(q_l) + J^T(q_l)F = \tau + \omega_l, \quad (1)$$

where $q_l \in \Re^n$ denotes the link angular positions, $M_l(q_l)$ the link inertia matrix, $C(q_l, \dot{q}_l)\dot{q}_l$ the centrifugal and Coriolis forces, $G(q_l)$ the gravity force, $J(q_l)$ the joint-space to task-space Jacobian matrix, $F \in \Re^n$ the task-space generalized forces on an environmental constraint exerted by the end-effector, τ the torque inputs, and ω_l the finite energy (i.e., $\omega_l \in L_{2e}$) unknown disturbances.

Note that $M_l(q_l), C(q_l, \dot{q}_l)\dot{q}_l, G(q_l), J(q)$, and F are not exactly known. Thus, estimates of these terms are used for control law construction. Let $\hat{M}_l(q_l), \hat{C}(q_l, \dot{q}_l)\dot{q}_l, \hat{G}(q_l), \hat{J}(q)$, and $\hat{F}$ denote the estimates of these terms, respectively; then, (1) can be rewritten as

$$\hat{M}_l(q_l)\ddot{q}_l + \hat{C}(q_l, \dot{q}_l)\dot{q}_l + \hat{G}(q_l) + \hat{J}^T(q_l)\hat{F} = \tau + \omega_\tau \quad (2)$$

where, $\omega_\tau = \tilde{M}_l(q_l)\ddot{q}_l + \tilde{C}(q_l, \dot{q}_l)\dot{q}_l + \tilde{G}(q_l) - \tilde{J}^T(q_l)F - \hat{J}^T(q_l)\tilde{F} + \omega_l$, $\tilde{J} = \hat{J} - J$, $\tilde{M}_l(q_l) = \hat{M}_l(q_l) - M_l(q_l)$, $\tilde{C}(q_l, \dot{q}_l) = \hat{C}(q_l, \dot{q}_l) - C(q_l, \dot{q}_l)$, $\tilde{G}(q_l) = \hat{G}(q_l) - G(q_l)$ and $\tilde{F} = \hat{F} - F$.

B. Environmental Modelling

The environmental constraints considered in this paper are very stiff but not perfectly rigid, frictionless surfaces with geometrical shapes which are not exactly known. For developing the required task-space reduced-order position dynamics and the algebraic constraint force description, several assumptions similar to those presented in [5] and [10] are made. These assumptions are as follows.

(A1) There exists a C^1 mapping $\hat{h}$ such that task-space variables $x \in \Re^n$ can be described as $x = \hat{h}(q_l) + \tilde{h}(q_l)$, where $\tilde{h}(q_l)$ represents the uncertainty with the length of the manipulator links. Further, the nominal joint-space to task-space Jacobian matrix $\hat{J} = (\partial\hat{h}/\partial q_l)(q_l) \in \Re^{n\times n}$ is nonsingular. Here, $x = [x_1^T \;\; x_2^T]^T$ with $x_1 \in \Re^m, x_2 \in \Re^k$, and $m + k = n \le 6$.

(A2) The nominal part of an uncertain constraint surface can be described by a holonomic relationship $\hat{\theta}(x) = 0_{k\times 1}$. Further, the true constraint surface can be described as $\hat{\theta}(x) = \omega_\theta$, where ω_θ is used to represent the uncertainties concerning the geometry and rigidity of the constraint.

(A3) $\Pi = (\partial\hat{\theta}/\partial x_2) \in \Re^{k\times k}$ is nonsingular. Therefore

$$\hat{A} = [\Sigma \quad \Pi] \tag{3}$$

has full rank, where $\Sigma = (\partial\hat{\theta}/\partial x_1) \in \Re^{k\times m}$.

(A4) From Assumptions (A2) and (A3) and the Implicit Function Theorem, there exists a unique C^1 mapping Ω such that $x_2 = \Omega(x_1)$ holds for the nominal holonomic constraint in Assumption (A2). Therefore, we have $x_2 = \Omega(x_1) + \omega_\Omega$ for the true constraint surface, where ω_Ω proceeds from $\omega_{\theta y}$. Also, it is assumed that $\Omega(x_1)$ and $\Gamma_{k\times m} = \partial\Omega(x_1)/\partial x_1$ are defined for all manipulator operations of interest. Differentiating the nominal holonomic constraint with respect to x_1, we obtain

$$\Sigma + \Pi\Gamma = 0_{k\times m}. \tag{4}$$

(A5) It is assumed that the end-effector is initially in contact with the constraint surface, and the control exercised over the constrained force is such that the force will always hold the end-effector on the constraint surface.

C. Decoupled Position Dynamics and Algebraic Force Model

It can be shown [5], [17], that the task-space generalized force F in (1) can be represented as

$$F = A\lambda = [\hat{A} + \tilde{A}]^T\lambda \quad \text{with } \hat{F} = \hat{A}^T\lambda$$

where $\hat{A}$ is given in (3), and $\tilde{A}$ results from $\omega_\theta; \lambda \in \Re^k$ represents the generalized force multipliers associated with the constraint. Now, (2) can be detailed further as

$$\hat{M}_l(q_l)\ddot{q}_l + \hat{C}(q_l,\dot{q}_l)\dot{q}_l + \hat{G}(q_l) + \hat{J}^T(q_l)\hat{A}^T\lambda = \tau + \omega_\tau. \tag{5}$$

For exploiting knowledge about a nominal holonomic constraint to formally decouple the dynamics of position from the effects of constraint force, several auxiliary treatments are required. Firstly, the coordinate transformation

$$u = \begin{bmatrix} u_1 \\ u_2 \end{bmatrix} = \begin{bmatrix} x_1 \\ x_2 - \Omega(x_1) \end{bmatrix} = \begin{bmatrix} x_1 \\ \omega_\Omega \end{bmatrix}$$

is adopted. Therefore, we have

$$x = \begin{bmatrix} x_1 \\ x_2 \end{bmatrix} = \begin{bmatrix} u_1 \\ u_2 + \Omega(u_1) \end{bmatrix}, \quad \dot{x} = S\dot{u}, \quad \text{and} \quad \ddot{x} = S\ddot{u} + \dot{S}\dot{u} \tag{6}$$

where

$$S = \frac{\partial x}{\partial u} = \begin{bmatrix} I_{m\times m} & 0_{m\times k} \\ \Gamma_{k\times m} & I_{k\times k} \end{bmatrix}.$$

Next, from Assumption (A1), we have $\dot{x} = [\hat{J}(q_l) + \tilde{J}(q_l)]\dot{q}_l$, where $\tilde{J}(q_l)$ results from $\tilde{h}(q_l)$. Therefore, $\dot{q}_l$ can be expressed as

$$\dot{q}_l = \hat{J}^{-1}(q_l)\dot{x} + \omega_J \tag{7}$$

where $\omega_J = -\hat{J}^{-1}(q_l)\tilde{J}(q_l)\dot{q}_l$. Differentiating (7) with respect to time, we have

$$\ddot{q}_l = \hat{J}^{-1}(q_l)\ddot{x} - \left[\hat{J}^{-1}(q_l)\dot{\hat{J}}(q_l,\dot{q}_l)\hat{J}^{-1}(q_l)\right]\dot{x} + \omega_{\dot{J}} \tag{8}$$

where $\omega_{\dot{J}} = -(d/dt)[\hat{J}^{-1}(q_l)\tilde{J}(q_l)\dot{q}_l]$. To simplify the notation, we shall omit the arguments of various functions (e.g., $\hat{J}^{-1}(\cdot), \dot{\hat{J}}(\cdot,\cdot)$, etc.) from now on.

Premultiplying (5) by $S^T\hat{J}^{-T}$ and using (6), (7), and (8), we obtain

$$\bar{M}\ddot{u} + \bar{C}\dot{u} + \bar{G} + S^T\hat{A}^T\lambda = \bar{B}\tau + \bar{B}\omega_x \tag{9}$$

where

$$\begin{aligned}
\bar{M} &= S^T\hat{J}^{-T}\hat{M}\hat{J}^{-T}S = \begin{bmatrix} \bar{M}_{11} & \bar{M}_{12} \\ \bar{M}_{21} & \bar{M}_{22} \end{bmatrix} \\
\bar{G} &= S^T\hat{J}^{-1}\hat{G} = \begin{bmatrix} \bar{G}_1 \\ \bar{G}_2 \end{bmatrix} \\
\bar{C} &= S^T\hat{J}^{-T}\left\{\hat{M}\hat{J}^{-1}\dot{S} + \left[\hat{C} - \hat{M}\hat{J}^{-1}\dot{\hat{J}}\right]\hat{J}^{-1}S\right\} \\
&= \begin{bmatrix} \bar{C}_{11} & \bar{C}_{12} \\ \bar{C}_{21} & \bar{C}_{22} \end{bmatrix} \\
\bar{B} &= S^T\hat{J}^{-T} = \begin{bmatrix} \bar{B}_1 \\ \bar{B}_2 \end{bmatrix}
\end{aligned}$$

and $\omega_x = \omega_\tau - \hat{M}\omega_{\dot{J}} - \hat{C}\omega_J$. By using (4) and rearranging the uncertain terms, (9) can be rewritten as

$$\begin{aligned}
\bar{M}\begin{bmatrix} \ddot{u}_1 \\ 0_{k\times 1} \end{bmatrix} + \bar{C}\begin{bmatrix} \dot{u}_1 \\ 0_{k\times 1} \end{bmatrix} + \begin{bmatrix} \bar{G}_1 \\ \bar{G}_2 \end{bmatrix} + \begin{bmatrix} 0_{m\times k} \\ \Pi^T \end{bmatrix}\lambda \\
= \begin{bmatrix} \bar{B}_1 \\ \bar{B}_2 \end{bmatrix}\tau + \omega_u
\end{aligned} \tag{10}$$

where

$$\omega_u = \bar{B}\omega_x - \bar{M}\begin{bmatrix} 0_{m\times 1} \\ \ddot{\omega}_\Omega \end{bmatrix} - \bar{C}\begin{bmatrix} 0_{m\times 1} \\ \dot{\omega}_\Omega \end{bmatrix} = \begin{bmatrix} \omega_u^1 \\ \omega_u^2 \end{bmatrix}.$$

From (10), a set of equations similar to the so-called reduced form [10] can be obtained as

$$\bar{M}_{11}\ddot{u}_1 + \bar{C}_{11}\dot{u}_1 + \bar{G}_1 = \bar{B}_1\tau + \omega_u^1 \tag{11}$$

$$\bar{M}_{21}\ddot{u}_1 + \bar{C}_{21}\dot{u}_1 + \bar{G}_2 + \Pi^T\lambda = \bar{B}_2\tau + \omega_u^2. \tag{12}$$

Equation (11) is the required task-space reduced-order position dynamics. For obtaining the required constraint force model, we first rewrite (11) as

$$\ddot{u}_1 = -\bar{M}_{11}^{-1}\left\{\bar{C}_{11}\dot{u}_1 + \bar{G}_1\right\} + \bar{M}_{11}^{-1}\bar{B}_1\tau + \bar{M}_{11}^{-1}\omega_u^1. \tag{13}$$

Next, let us substitute (13) into (12); then the algebraic constraint force model can be obtained as

$$\Pi^T \lambda + \left\{\bar{C}_{21} - \bar{M}_{21}\bar{M}_{11}^{-1}\bar{C}_{11}\right\}\dot{u}_1 + \left\{\bar{G}_2 - \bar{M}_{21}\bar{M}_{11}^{-1}\bar{G}_1\right\} = \left\{\bar{B}_2 - \bar{M}_{21}\bar{M}_{11}^{-1}\bar{B}_1\right\}\tau + \left\{\omega_u^2 - \bar{M}_{21}\bar{M}_{11}^{-1}\omega_u^1\right\} \quad (14)$$

Equations (11) and (14) will later be exploited for developing our adaptive $H\infty$ position/force tracking control scheme. In this control scheme, not only will model based knowledge according to the laws of physics be used to design the robust nonlinear $H\infty$ control, but also the information contained in the unknown parameters and unmodelled dynamics of the manipulator as well as that contained in the uncertainties with environmental modelling will be extracted by NN devices to further improve the tracking performance. For this latter purpose, two nonlinear mappings f_p and f_f are then defined. Let

$$f_p = \bar{M}_{11}^{-1}\omega_u^1 \quad (15)$$

$$f_f = \Pi^{-T}\left\{\omega_u^2 - \bar{M}_{21}\bar{M}_{11}^{-1}\omega_u^1\right\} \quad (16)$$

where f_p and f_f denote the lumped effects of both the structured/unstructured uncertainties of manipulator dynamics and the uncertainties of environmental modelling. f_p and f_f are the nonlinear mappings to be learned by NN devices.

III. Multilayered Feedforward Neural Networks

A three layered feedforward NN structure is adopted for learning both f_p and f_f. This NN structure uses linear units in its input/output layers and hyperbolic tangent neurones for its middle hidden layer. This means the activation function for the ith hidden unit is described by

$$\sigma_i(z_n) = \tanh(\alpha(\varphi(z_n) - c_i)) \quad (17)$$

where c_i represents the centre of this activation function, α a specified constant, and $\varphi(z_n)$ is a function of NN's input vector z_n. Only those weights that connect the hidden layer and the output layer are adjustable in the proposed NN structure. The other parameters, such as the weights connecting the input layer and the hidden layer, the centres of the hidden layer units, etc., are fixed after the NN device has been constructed. For such a NN device with j hidden units and n outputs, the kth NN output can be characterized as

$$F_k(z_n, \theta_k) = \xi^T \theta_k \quad (18)$$

where $\theta_k = [\theta_{k1} \ldots \theta_{kj}]^T$ represents the weights connecting the kth output and the hidden layer, and, $\xi = [\sigma_1(z_n) \ldots \sigma_j(z_n)]^T$ is the output vector of the hidden layer. Therefore, the operation of the whole NN device can be described as

$$F(z,\Theta) = \begin{bmatrix} F_1(z_n,\theta_1) \\ \vdots \\ F_n(z_n,\theta_n) \end{bmatrix} = \mathrm{diag}(\xi^T \cdots \xi^T)\begin{bmatrix} \theta_1 \\ \vdots \\ \theta_n \end{bmatrix} = \Xi\Theta. \quad (19)$$

It is well known that this type of NN structure has universal approximation capacity [18], [19]. This means that for any given real continuous mapping $g\colon \Omega_{z_n} \to \Re^s, \Omega_{z_n} \subseteq \Re^t$ and arbitrary $\varepsilon_{\mathrm{NN}} \geq 0$, there exists a multilayered feedforward NN device in the form of (19) with j^* units in the middle layer and a $\Theta = \breve{\Theta}$ such that $\sup_{z_n \in \Omega_{z_n}} \|F(z_n, \breve{\Theta}) - g(z_n)\| \leq \varepsilon_{\mathrm{NN}}$. However, in this paper, it is assumed that we do not have any further knowledge about the finite energy disturbances ω_l. This means the arguments for disturbance mappings ω_l are not known; therefore, the universal approximation theorem [18], [19] cannot be directly used for learning f_p and f_f.

To extend the ability of the proposed NN structure for extracting the information contained in the structured/unstructured manipulator uncertainties and in the uncertainties of environmental modelling, a couple of auxiliary analyses are required. Firstly, let $F_p(z_p, \Theta_p)$ and $F_f(z_f, \Theta_f)$ in the form of (19) be the selected NN devices to learn f_p and f_f, respectively. Then, as indicated in [20], the ideal constant approximation parameters for $F_p(z_p, \Theta_p)$ and $F_f(z_f, \Theta_f)$ can be defined as

$$\Theta_p^* = \arg \min_{\Theta_p \in \Omega_{\Theta_p}} \max_{z_p \in \Omega_{z_p}} \|F_p(z_p, \Theta_p) - f_p\| \quad (20)$$

$$\Theta_f^* = \arg \min_{\Theta_f \in \Omega_{\Theta_f}} \max_{z_f \in \Omega_{z_f}} \|F_f(z_f, \Theta_f) - f_f\| \quad (21)$$

where $\Omega_{\Theta_p}, \Omega_{\Theta_f}, \Omega_{z_p}$ and Ω_{z_f} denote the compact sets of suitable bounds of the NN weight vectors Θ_p and Θ_f, and the NN input vectors z_p and z_f, respectively. Now, the goal of the adopted NN devices $F_p(z_p, \Theta_p)$ and $F_f(z_f, \Theta_f)$ is to learn the ideal mappings $F_p(z_p, \Theta_p^*)$ and $F_f(z_f, \Theta_f^*)$, where Θ_p^* and Θ_f^* are as defined in (20) and (21), respectively.

Then, according to the above definitions, f_p and f_f can be rewritten as

$$f_p = \Xi_p(z_p)\hat{\Theta}_p - \Xi_p(z_p)\tilde{\Theta}_p + \varepsilon_p \quad (22)$$

$$f_f = \Xi_f(z_f)\hat{\Theta}_f - \Xi_f(z_f)\tilde{\Theta}_f + \varepsilon_f \quad (23)$$

where $\tilde{\Theta}_p = \hat{\Theta}_p - \Theta_p^*$ and $\tilde{\Theta}_f = \hat{\Theta}_f - \Theta_f^*$. $\hat{\Theta}_p$ and $\hat{\Theta}_f$ represent the estimates of Θ_p^* and Θ_f^*, respectively; and $\varepsilon_p, \varepsilon_f$ denote the optimal approximation error mappings for the selected NN devices $F_p(\cdot,\cdot)$ and $F_f(\cdot,\cdot)$. Equations (22) and (23) will be used to design the updating laws of NN weights in our later discussion.

IV. Adaptive $H\infty$ Neural Networks Position/Force Tracking Controller

The control objectives considered in this paper are to make the motion of the end-effector track a desired path u_{1d}, with $\dot{u}_{1d}$ and $\ddot{u}_{1d}$ being continuous, as well as to make the contact force λ track a desired sufficiently smooth trajectory λ_d. Besides, a $H\infty$ performance requirement is to be satisfied by the closed loop system. This $H\infty$ performance is represented in terms of a finite L_2 gain relationship [21], [22].

Definition 1 (Finite Gain [21], [22]): Let $\rho \geq 0$. System $y = Gu$ is said to have L_2 gain less than or equal to ρ, if $\exists \beta \in \Re$ such that

$$\int_0^T \|y(t)\|^2 \, dt \leq \rho^2 \int_0^T \|u(t)\|^2 \, dt + \beta$$

holds $\forall u \in L_{2e}, \forall T \in \Re^+$.

To achieve the above control objectives, it is necessary to develop a suitable error dynamic system that can be exploited for the control design. Let the torque input be set as

$$\tau = \begin{bmatrix} \bar{B}_1 \\ \bar{B}_2 - \bar{M}_{21}\bar{M}_{11}^{-1}\bar{B}_1 \end{bmatrix}^{-1} \begin{bmatrix} \Lambda_p \\ \Lambda_f \end{bmatrix} \tag{24}$$

where

$$\begin{aligned} \Lambda_p = {} & \bar{M}_{11}\left[\ddot{u}_{1d} - K_v\dot{e}_{u1} - K_p e_{u1} + v_p - \Xi_p\hat{\Theta}_p\right] \\ & + \bar{C}_{11}\dot{u}_1 + \bar{G}_1 \end{aligned} \tag{25}$$

$$\begin{aligned} \Lambda_f = {} & \Pi^T\left[\lambda_d + z + v_\lambda - \Xi_f\hat{\Theta}_f\right] \\ & + \left[\bar{C}_{21} - \bar{M}_{21}\bar{M}_{11}^{-1}\bar{C}_{11}\right]\dot{u}_1 + \left[\bar{G}_2 - \bar{M}_{21}\bar{M}_{11}^{-1}\bar{G}_1\right] \end{aligned} \tag{26}$$

and the dynamic of z is selected to be

$$\dot{z} = -\mu_z z - \alpha_z e_\lambda \tag{27}$$

with $\mu_z, \alpha_z \in \Re^+$, being the design parameters to be chosen. Here, $e_{u1} = u_1 - u_{1d}, \dot{e}_{u1} = \dot{u}_1 - \dot{u}_{1d}$, and $e_\lambda = \lambda - \lambda_d$. The v_p and v_λ are the robustifying terms for the position sub-controller Λ_p and the force sub-controller Λ_f, respectively; $\Xi_p\hat{\Theta}_p$ denotes the knowledge about f_p learned by $F_p(\cdot,\cdot)$, and $\Xi_f\hat{\Theta}_f$ the knowledge about f_f learned by $F_f(\cdot,\cdot)$. Also, in $\Lambda_p, K_v > 0$ and $K_p > 0$ are diagonal matrices and play a similar role as in the standard computed torque (CT) controllers of the motion control problem.

Defining

$$x_p = \begin{bmatrix} e_{u1} \\ \dot{e}_{u1} \end{bmatrix}$$

and applying (24)–(27) to system (11) and (14), we have

$$e_\lambda = z + v_\lambda - \Xi_f\tilde{\Theta}_f + \varepsilon_f \tag{28}$$

$$\dot{x}_p = A_p x_p + B_p v_p - B_p\Xi_p\tilde{\Theta}_p + B_p\varepsilon_p \tag{29}$$

where

$$A_p = \begin{bmatrix} 0 & I_{m\times m} \\ -K_p & -K_v \end{bmatrix}$$

and

$$B_p = \begin{bmatrix} 0 \\ I_{m\times m} \end{bmatrix}.$$

Equation (29) is the error system for the task-space reduced-order position dynamics, and (27) and (28) represent the error system with the contact force.

Instead of separately developing $H\infty$ control schemes for the position sub-controller Λ_p and the force sub-controller Λ_f (as in the hybrid control approach), we shall design all control laws simultaneously by using a storage function. Based on the whole error system (27)–(29), the following results can be concluded.

Theorem 1 (Adaptive $H\infty$ NN Position/Force Tracking Controller): If the dynamics of z (27) has been set to have $\alpha_z = 2$ and $\mu_z \in \Re^+$, as well as the torque input τ in (24), the updating laws of NN weights

$$\dot{\hat{\Theta}}_p = \gamma_1\Xi_p^T B_p^T P_p x_p \tag{30}$$

$$\dot{\hat{\Theta}}_f = \gamma_2\Xi_f^T e_\lambda \tag{31}$$

and the robustifying control laws

$$v_\lambda = -\frac{\beta_\lambda}{2}e_\lambda \tag{32}$$

$$v_p = -R_p^{-1}B_p^T P_p x_p. \tag{33}$$

are used for the constrained n-link manipulator system (1), then the $H\infty$ tracking performance

$$\begin{aligned} & \int_0^T \left\{\|x_p\|_{Q_p}^2 + \alpha_\lambda\|e_\lambda\|^2 + \frac{\alpha_\lambda\mu_z}{1+\beta_\lambda}\|z\|^2\right\} dt \\ & \le \rho^2\int_0^T \left\{\|\varepsilon_p\|^2 + \|\varepsilon_f\|^2\right\} dt + \beta_a \end{aligned} \tag{34}$$

is achieved for a prescribed level ρ, where $\alpha_\lambda > \rho^2$ is the weighting scalar for $e_\lambda, Q_p^T = Q_p > 0$ the weighting matrix for $x_p, (\alpha_\lambda\mu_z/1+\beta_\lambda) \in \Re^+$ the weighting scalar for z and $\beta_a \in \Re$. Also, in (30)–(33), $\beta_\lambda \ge (\alpha_\lambda/\rho^2) - 1 > 0, R_p^T = R_p > 0$, and $P_p^T = P_p > 0$ is the solution of the Riccati-like equation

$$\begin{aligned} & A_p^T P_p + P_p A_p - P_p B_p\left[2R_p^{-1} - \frac{I_{m\times m}}{\rho^2}\right]B_p^T P_p \\ & + Q_p = 0_{2m\times 2m}. \end{aligned} \tag{35}$$

Proof: Let us select a storage function candidate

$$\begin{aligned} V = {} & x_p^T P_p x_p + \frac{\alpha_\lambda}{2[1+\beta_\lambda]}z^T z + \frac{1}{\gamma_1}\tilde{\Theta}_p^T\tilde{\Theta}_p \\ & + \frac{\alpha_\lambda}{\gamma_2[1+\beta_\lambda]}\tilde{\Theta}_f^T\tilde{\Theta}_f. \end{aligned} \tag{36}$$

Differentiating the above equation yields

$$\begin{aligned} \dot{V} = {} & \dot{x}_p^T P_p x_p + x_p^T P_p\dot{x}_p + \frac{\alpha_\lambda}{1+\beta_\lambda}\dot{z}^T z \\ & + \frac{2}{\gamma_1}\dot{\tilde{\Theta}}_p^T\tilde{\Theta}_p + \frac{2\alpha_\lambda}{\gamma_2[1+\beta_\lambda]}\dot{\tilde{\Theta}}_f^T\tilde{\Theta}_f. \end{aligned} \tag{37}$$

By (27)–(29) and the facts that $\dot{\tilde{\Theta}}_p = \dot{\hat{\Theta}}_p$ and $\dot{\tilde{\Theta}}_f = \dot{\hat{\Theta}}_f$, the above equation becomes

$$\begin{aligned} \dot{V} = {} & x_p^T A_p^T P_p x_p + x_p^T P_p A_p x_p + 2x_p^T P_p B_p v_p \\ & + 2x_p^T P_p B_p\varepsilon_p - 2x_p^T P_p B_p\Xi_p\tilde{\Theta}_p \\ & - \frac{\alpha_\lambda\mu_z}{1+\beta_\lambda}\|z\|^2 - \frac{\alpha_\lambda\alpha_z}{1+\beta_\lambda}e_\lambda^T\left[e_\lambda - v_\lambda + \Xi_f\tilde{\Theta}_f - \varepsilon_f\right] \\ & + \frac{2}{\gamma_1}\dot{\hat{\Theta}}_p^T\tilde{\Theta}_p + \frac{2\alpha_\lambda}{\gamma_2[1+\beta_\lambda]}\dot{\hat{\Theta}}_f^T\tilde{\Theta}_f. \end{aligned} \tag{38}$$

From (30)–(33), the Riccati-like (35), and $\alpha_z = 2$, we obtain

$$\begin{aligned} \dot{V} = {} & -\|x_p\|_{Q_p}^2 + \rho^2\|\varepsilon_p\|^2 - \left\|\rho\varepsilon_p - \frac{1}{\rho}B_p^T P_p x_p\right\|^2 \\ & - \frac{\alpha_\lambda\mu_z}{1+\beta_\lambda}\|z\|^2 - \alpha_\lambda\|e_\lambda\|^2 + \frac{\alpha_\lambda}{1+\beta_\lambda}\|\varepsilon_f\|^2 - \frac{\alpha_\lambda}{1+\beta_\lambda}\|\varepsilon_f - e\lambda\|^2 \\ \le {} & -\|x_p\|_{Q_p}^2 - \alpha_\lambda\|e_\lambda\|^2 - \frac{\alpha_\lambda\mu_z}{1+\beta_\lambda}\|z\|^2 + \rho^2\|\varepsilon_p\|^2 \\ & + \rho^2\|\varepsilon_f\|^2. \end{aligned} \tag{39}$$

Integrating the above equation from $t=0$ to $t=T$ yields

$$V(T)-V(0)\le -\int_0^T\left[\|x_p\|_{Q_p}^2+\alpha_\lambda\|e_\lambda\|^2+\frac{\alpha_\lambda\mu_z}{1+\beta_\lambda}\|z\|^2\right]dt + \rho^2\int_0^T\left[\|\varepsilon_p\|^2+\|\varepsilon_f\|^2\right]\,dt.$$

Since $V(T)\ge 0$, the above inequality implies the following inequality

$$\int_0^T\left[\|x_p\|_{Q_p}^2+\alpha_\lambda\|e_\lambda\|^2+\frac{\alpha_\lambda\mu_z}{1+\beta_\lambda}\|z\|^2\right]dt \le \rho^2\int_0^T\left[\|\varepsilon_p\|^2+\|\varepsilon_f\|^2\right]\,dt+V(0).$$

This is (34). $\square$

Remark 1: The $H\infty$ tracking performance in (34) does not explicitly take any control effort into consideration. Therefore, this is a singular $H\infty$ performance requirement. The control efforts of the robustifying terms v_p and v_f can be taken into account as well. In this case, the augmented $H\infty$ tracking performance becomes

$$\int_0^T\left\{\|x_p\|_{Q_p}^2+\alpha_\lambda\|e_\lambda\|^2+\frac{\alpha_\lambda\mu_z}{1+\beta_\lambda}\|z\|^2+\|v_p\|_{R_p}^2 + \frac{\alpha_\lambda}{\beta_\lambda[1+\beta_\lambda]}\|v_\lambda\|^2\right\}dt \le \rho^2\int_0^T\left\{\|\varepsilon_p\|^2+\|\varepsilon_f\|^2\right\}\,dt+\beta_a.$$

Further, the required modifications are to change the Riccati-like equation (35) to

$$A_p^TP_p+P_pA_p - P_pB_p\left[R_p^{-1}-\frac{I_{m\times m}}{\rho^2}\right]B_p^TP_p+Q_p=0_{2m\times 2m} \quad (40)$$

and to change (32) to

$$v_\lambda=-\beta_\lambda e_\lambda. \quad (41)$$

Remark 2: It is worth noting that exact knowledge about Ω_{Θ_p} and Ω_{Θ_f} in (20) and (21) is not required to make the proposed control scheme successful. Whenever the explicit specifications on Ω_{Θ_p} and Ω_{Θ_f} are required, the following Projection algorithms [23] can be used to achieve this purpose. Let us assume that the required compact sets Ω_{Θ_p} and Ω_{Θ_f} are specified as $\Omega_{\Theta_p}:=\{\Theta_p|\|\Theta_p\|\le d_p\}$ and $\Omega_{\Theta_f}:=\{\Theta_f|\|\Theta_f\|\le d_f\}$, where d_p and d_f are positive constants. Then, the updating laws of NN weights (30)–(31) should be modified as

$$\dot{\hat{\Theta}}_p=\gamma_1\Xi_p^TB_p^TP_px_p+c_p\frac{\gamma_1x_p^TP_pB_p\Xi_p\hat{\Theta}_p}{d_p^2}\hat{\Theta}_p,$$

$$c_p=\begin{cases}-1 & \text{if } \|\hat{\Theta}_p\|=d_p \quad \text{and} \quad x_p^TP_pB_p\Xi_p\hat{\Theta}_p>0\\ 0 & \text{otherwise}\end{cases}$$

$$\dot{\hat{\Theta}}_f=\gamma_2\Xi_f^Te_\lambda+c_f\frac{\gamma_2e_\lambda^T\Xi_f\hat{\Theta}_f}{d_f^2}\hat{\Theta}_f,$$

$$c_f=\begin{cases}-1 & \text{if } \|\hat{\Theta}_f\|=d_f \quad \text{and} \quad e_\lambda^T\Xi_f\hat{\Theta}_f>0\\ 0 & \text{otherwise.}\end{cases}$$

Under these modified updating laws, it can be shown that if $\|\Theta_p(0)\|\le d_p$ then $\|\Theta_p(t)\|\le d_p$ for $\forall t>0$, and if $\|\Theta_f(0)\|\le d_f$ then $\|\Theta_f(t)\|\le d_f$ for $\forall t\ge 0$. Also, it can be validated that the $H\infty$ tracking performance (34) is still satisfied.

Remark 3: In Theorem 1, α_z was chosen to be 2 such that the $H\infty$ tracking performance (34) can be acheived for a prescribed level ρ. α_z can be arbitrarily positive real number (i.e., $\alpha_z\in\Re^+$). In this case, by choosing $\alpha_\lambda>2\rho^2/\alpha_z$ and $\beta_\lambda\ge\alpha_\lambda\alpha_z/2\rho^2-1>0$, the closed-loop system can have the $H\infty$ tracking performance

$$\int_0^T\left\{\|x_p\|_{Q_p}^2+\frac{\alpha_\lambda\alpha_z}{2}\|e_\lambda\|^2+\frac{\alpha_\lambda\mu_z}{1+\beta_\lambda}\|z\|^2\right\}dt \le \rho^2\int_0^T\left\{\|\varepsilon_p\|^2+\|\varepsilon_f\|^2\right\}\,dt+\beta_a$$

achieved for a prescribed level ρ.

Remark 4: As indicated in [24], the Riccati-like equation

$$A_p^TP_p+P_pA_p - P_pB_p\left[2R_p^{-1}-\frac{I_{m\times m}}{\rho^2}\right]B_p^TP_p+Q_p=0_{2m\times 2m}$$

can have a symmetric positive definite solution $P_p^T=P_p0$ if and only if

$$2\rho^2I_{m\times m}>R_p.$$

Therefore, for a selected weighting $R_p^T=R_p>0$ in control law $v_p=-R_p^{-1}B_p^TP_px_p$, inequality $2\rho^2I_{m\times m}>R_p$ give the lower bound for ρ in the $H\infty$ tracking performance (34).

For explicating the control scheme in Theorem 1, let us firstly rewrite the position sub-controller Λ_p in (25) as

$$\Lambda_p=\Lambda P_{\rm CT}+\Lambda P_{\rm NN}+\Lambda P_v \quad (42)$$

where

$$\Lambda P_{\rm CT}=\bar{M}_{11}\left[\ddot{u}_{1d}-K_v\dot{e}_{u1}-K_pe_{u1}\right]+\bar{C}_{11}\dot{u}_1+\bar{G}_1 \quad (43)$$

is the CT-like controller in this position sub-controller, and

$$\Lambda P_{\rm NN}=-\bar{M}_{11}\Xi_p\hat{\Theta}_p \quad (44)$$

$$\Lambda P_v=-\bar{M}_{11}R_p^{-1}B_p^TP_px_p \quad (45)$$

are the NN controller and the embedded robustifying controller for this Λ_p, respectively.

Next, the force sub-controller Λ_f in (26) is rewritten as

$$\Lambda_f=\Lambda F_{\rm CT}+\Lambda F_{\rm NN}+\Lambda F_v \quad (46)$$

where

$$\Lambda F_v=-\frac{\beta_\lambda}{2}\Pi^Te_\lambda \quad (47)$$

$$\Lambda F_{\rm NN}=-\Pi^T\Xi_f\hat{\Theta}_f \quad (48)$$

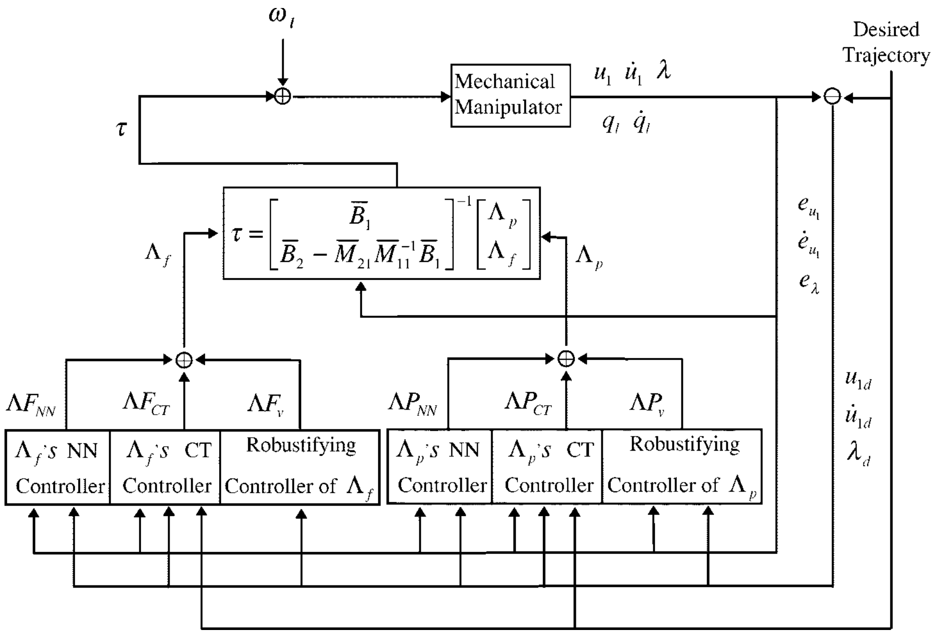

Fig. 1. Adaptive $H\infty$ NN Position/Force Control Structure.

are the embedded robustifying controller and the NN controller for this Λ_f, respectively;

$$\Lambda F_{\rm CT} = \Pi^T[\lambda_d + z] + \left[\bar{C}_{21} - \bar{M}_{21}\bar{M}_{11}^{-1}\bar{C}_{11}\right]\dot{u}_1 + \left[\bar{G}_2 - \bar{M}_{21}\bar{M}_{11}^{-1}\bar{G}_1\right] \tag{49}$$

with

$$\dot{z} = -\mu_z z - \alpha_z e_\lambda \tag{50}$$

is the CT-like controller in this Λ_f.

According to these defined terms, the control scheme in Theorem 1 is depicted in Fig. 1.

V. Suboptimal $H\infty$ Position/Force Tracking Controller

In this section, we aim to show that the learning capacity of NN devices in Theorem 1 deserves to be implanted into its associated suboptimal $H\infty$ only position/force tracking control scheme. For this purpose, the following two steps are taken. Firstly, the suboptimal $H\infty$ only position/force tracking control scheme is derived in Theorem 2. This $H\infty$ only controller is the counterpart of the adaptive $H\infty$ NN position/force tracking control scheme in Theorem 1. Secondly, the comparison of the upper bound on $H\infty$ tracking performance index between these two $H\infty$ based position/force tracking control schemes is given in Theorem 3.

In the following, the suboptimal $H\infty$ only controller for the simultaneous position/force tracking control of constrained manipulator is developed. As before, we begin with formulating the required error system. For this purpose and the fact that NN devices will be absent in this control scheme, the torque input (24) is modified to be (51), shown at the bottom of the page, with (27) still being used for the dynamics of z. Next, applying (27) and (51) to system (11) and (14) gives

$$e_\lambda = z + v_\lambda + f_f \tag{52}$$

$$\dot{x}_p = A_p x_p + B_p v_p + B_p f_p. \tag{53}$$

Equation (53) is the required error system for position dynamics, and (27) and (52) are the error system for the contact force. Based on the whole error system (27) and (52) and (53), the following results can be concluded.

Theorem 2 (Suboptimal $H\infty$ Position/Force Tracking Controller): If the dynamics of z (27) has been set to have $\alpha_z = 2$ and $\mu_z \in \Re^+$, and the robustifying control laws (32) and (33) are used for (51), then the H_∞ tracking performance

$$\int_0^T \left\{ \|x_p\|_{Q_p}^2 + \alpha_\lambda \|e_\lambda\|^2 + \frac{\alpha_\lambda \mu_z}{1+\beta_\lambda}\|z\|^2 \right\} dt \le \rho^2 \int_0^T \{\|f_p\|^2 \|f_f\|^2\} \, dt + \beta_h \tag{54}$$

of the closed loop system (27), (32), (33), (51), and (1) is achieved for a prescribed level ρ, where $\alpha_\lambda > \rho^2$ is the weighting scalar for e_λ, $Q_p^T = Q_p > 0$ the weighting matrix for x_p, $\alpha_\lambda \mu_z / 1 + \beta_z$ the weighting scalar for z and $\beta_h \in \Re$. Also, $\beta_\lambda \ge (\alpha_\lambda/\rho^2) - 1 > 0$, $R_p^T = R_p > 0$, and $P_p^T = P_p > 0$ is the solution of the Riccati-like equation (35).

$$\tau = \begin{bmatrix} \bar{B}_1 \\ \bar{B}_2 - \bar{M}_{21}\bar{M}_{11}^{-1}\bar{B}_1 \end{bmatrix}^{-1} \times \begin{bmatrix} \bar{M}_{11}[\ddot{u}_{1d} - K_v \dot{e}_{u1} - K_p e_{u1} + v_p] + \bar{C}_{11}\dot{u}_1 + \bar{G}_1 \\ \Pi^T[\lambda_d + z + v_\lambda] + \left[\bar{C}_{21} - \bar{M}_{21}\bar{M}_{11}^{-1}\bar{C}_{11}\right]\dot{u}_1 + \left[\bar{G}_2 - \bar{M}_{21}\bar{M}_{11}^{-1}\bar{G}_1\right] \end{bmatrix} \tag{51}$$

Proof: Let us select a storage function candidate

$$V = x_p^T P_p x_p + \frac{\alpha_\lambda}{2[1+\beta_\lambda]} z^T z. \tag{55}$$

Differentiating the above equation yields

$$\dot{V} = \dot{x}_p^T P_p x_p + x_p^T P_p \dot{x}_p + \frac{\alpha_\lambda}{[1+\beta_\lambda]} \dot{z}^T z. \tag{56}$$

By (27) and (52)–(53), the above equation becomes

$$\begin{aligned} \dot{V} &= x_p^T A_p^T P_p x_p + x_p^T P_p A_p x_p \\ &\quad + 2x_p^T P_p B_p v_p + 2x_p^T P_p B_p f_p \\ &\quad - \frac{\alpha_\lambda \mu_z}{1+\beta_\lambda}\|z\|^2 - \frac{\alpha_\lambda \alpha_z}{1+\beta_\lambda} e_\lambda^T [e_\lambda - v_\lambda - f_f]. \end{aligned} \tag{57}$$

From (32)–(33) with $\alpha_z = 2$, we get

$$\begin{aligned} \dot{V} &= -\|x_p\|_{Q_p}^2 + \rho^2\|f_p\|^2 - \left\|\rho f_p - \frac{1}{\rho} B_p^T P_p x_p\right\|^2 \\ &\quad - \frac{\alpha_\lambda \mu_z}{1+\beta_\lambda}\|z\|^2 - \alpha_\lambda \|e_\lambda\|^2 \\ &\quad + \frac{\alpha_\lambda}{1+\beta_\lambda}\|f_f\|^2 - \frac{\alpha_\lambda}{1+\beta_\lambda}\|f_f - e_\lambda\|^2 \\ &\le -\|x_p\|_{Q_p}^2 - \alpha_\lambda\|e_\lambda\|^2 - \frac{\alpha_\lambda \mu_z}{1+\beta_\lambda}\|z\|^2 \\ &\quad + \rho^2\|f_p\|^2 + \rho^2\|f_f\|^2. \end{aligned} \tag{58}$$

By the similar procedure to the proof of Theorem 1, the proof is obtained. □

Now, we will show that the H_∞ tracking performance in Theorem 2, $\int_0^T \{\|x_p\|_{Q_p}^2 + \alpha_\lambda\|e_\lambda\|^2 + (\alpha_\lambda \mu_z/1+\beta_\lambda)\|z\|^2\}\, dt$, can be improved via the NN's adaptive learning mechanism in Theorem 1, if the adopted NN devices can effectively approximate f_p and f_f in the sense that the magnitudes and increasing rates of accumulating approximation errors $\int_0^T \|\varepsilon_p\|^2\, dt$ and $\int_0^T \|\varepsilon_f\|^2\, dt$ can be rendered smaller than those of $\int_0^T \|f_p\|^2\, dt$ and $\int_0^T \|f_f\|^2\, dt$, respectively.

Assumption (A6): The adopted NN devices $F_p(z_p, \Theta_p)$ and $F_f(z_f, \Theta_f)$ are effective in learning f_p and f_f. This means that $\int_0^T \|\varepsilon_p(t)\|^2\, dt < \int_0^T \|f_p(t)\|^2\, dt$ and $\int_0^T \|\varepsilon_f(t)\|^2\, dt < \int_0^T \|f_f(t)\|^2\, dt\ \forall T > 0$, as well as both $\int_0^T \{\|f_p(t)\|^2 - \|\varepsilon_p(t)\|^2\}\, dt$ and $\int_0^T \{\|f_f(t)\|^2 - \|\varepsilon_f(t)\|^2\}\, dt$ are monotone increasing functions with respect to $T > 0$.

Theorem 3: Suppose Assumption (A6) holds, then the upper bound on the $H\infty$ tracking performance of the adaptive $H\infty$ NN position/force tracking control law in Theorem 1 will ultimately be smaller than that of the suboptimal $H\infty$ only position/force tracking control law in Theorem 2.

Proof: From Assumption (A6), we have

$$\begin{aligned} \int_0^T &\{[\|f_p(t)\|^2 + \|f_f(t)\|^2] \\ &- [\|\varepsilon_p(t)\|^2 + \|\varepsilon_f(t)\|^2]\}\, dt > 0, \quad \forall T > 0 \end{aligned} \tag{59}$$

which is a monotone increasing function with respect to $T > 0$.

Inequality (59) and the monotone increasing property of

$$\int_0^T \{[\|f_p(t)\|^2 + \|f_f(t)\|^2] - [\|\varepsilon_p(t)\|^2 + \|\varepsilon_f(t)\|^2]\}\, dt$$

lead to

$$\begin{aligned} \rho^2 &\int_0^T [\|\varepsilon_p(t)\|^2 + \|\varepsilon_f(t)\|^2]\, dt + \beta_a \\ &< \rho^2 \int_0^T [\|f_p(t)\|^2 + \|f_f(t)\|^2]\, dt + \beta_h \\ &\qquad \forall T > \bar{T} \ge 0 \end{aligned} \tag{60}$$

where $\bar{T} = 0$ whenever $\beta_h \ge \beta_a$, and $\bar{T}$ is the time that

$$\begin{aligned} \rho^2 &\int_0^{\bar{T}} [\|\varepsilon_p(t)\|^2 + \|\varepsilon_f(t)\|^2]\, dt + \beta_a \\ &- \rho^2 \int_0^{\bar{T}} [\|f_p(t)\|^2 + \|f_f(t)\|^2]\, dt - \beta_h = 0 \end{aligned}$$

happens whenever $\beta_h < \beta_a$. Inequality (60) shows that the right-hand side of (34) will be eventually smaller than that of (54). Thus, this theorem is proved. □

Remark 5: The proof of Theorem 3 says that, after a finite period of learning, the adaptive $H\infty$ NN position/force tracking control law in Theorem 1 can eventually be less conservative than its counterpart suboptimal $H\infty$ only position/force tracking control law in Theorem 2, whenever the constructed NN devices $F_p(\cdot,\cdot)$ and $F_f(\cdot,\cdot)$ are effective. In other words, the total energy of the uncertain mapping to be attenuated in the adaptive $H\infty$ NN tracking control scheme of Theorem 1, $\int_0^T [\|\varepsilon_p\|^2 + \|\varepsilon_f\|]^2\, dt + (\beta_a/\rho^2)$, will eventually be smaller than that of the suboptimal $H\infty$ only tracking control scheme in Theorem 2, whenever $F_p(\cdot,\cdot)$ and $F_f(\cdot,\cdot)$ are effective.

VI. Simulation Study

To evaluate the proposed control scheme, the dynamics of a constrained planar two-link mechanical arm, shown in Fig. 2, is simulated. With respect to this mechanical manipulator, the matrices in the dynamic equation (1) are given by

$$\begin{aligned} M_l &= \begin{bmatrix} (m_1+m_2)l_1^2 + m_2 l_2^2 + 2m_2 l_1 l_2 c_2 & m_2 l_2^2 + m_2 l_1 l_2 c_2 \\ m_2 l_2^2 + m_2 l_1 l_2 c_2 & m_2 l_2^2 \end{bmatrix} \\ C &= m_2 l_1 l_2 s_2 \begin{bmatrix} -\dot{q}_2 & -(\dot{q}_1 + \dot{q}_2) \\ -\dot{q}_1 & 0 \end{bmatrix} \\ G &= g \begin{bmatrix} (m_1+m_2) l_1 c_1 + m_2 l_2 c_{12} \\ m_2 l_2 c_{12} \end{bmatrix} \\ J &= \begin{bmatrix} -l_1 s_1 - l_2 s_{12} & -l_2 s_{12} \\ l_1 c_1 + l_2 c_{12} & l_2 c_{12} \end{bmatrix} \end{aligned}$$

where $g = 9.8$ (m/s^2) is the acceleration of gravity, q_1 and q_2 (rad) the link angular positions, m_1 and m_2 (kg) the link masses, l_1 and l_2 (m) the link lengths, as well as $c_1 = \cos(q_1), c_{12} = \cos(q_1 + q_2)$, and so on.

This manipulator is assumed to be in contact with a surface S_1 shown in Fig. 2. This surface has a not exactly known slope

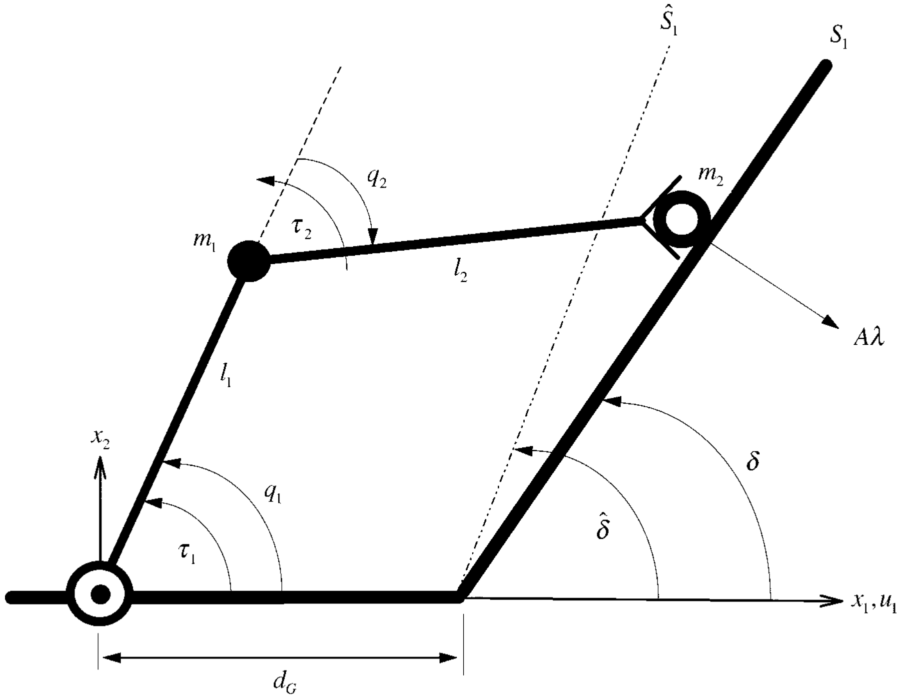

Fig. 2. Constrained planar two-link mechanical arm.

δ (rad), and can be described as $x_2 = (x_1 - d_G)\tan(\delta)$, where the horizontal distance d_G (m) is assumed to be equal to 0.8. In addition, the surface S_1 is assumed to be very rigid, with a stiffness constant 10^5 (N/m).

In this simulation, the uncertain parameters of the constrained manipulator system are assumed to have the true values

$$m_1 = 1.2, \quad m_2 = 1.1, \quad l_1 = 1.02724, \quad l_2 = 0.98041, \quad \delta = \frac{91}{360}\pi$$

and the estimated nominal values of these parameters are taken to be

$$\hat{m}_1 = 1.5, \quad \hat{m}_2 = 1, \quad \hat{l}_1 = \hat{l}_2 = 1, \quad \hat{\delta} = \frac{\pi}{4}.$$

For illustration, the parameters in the proposed adaptive $H\infty$ NN controller are taken to be

$$\rho = 0.6, \quad \mu_z = 100, \quad K_p = 18, \quad K_v = 9, \quad \alpha_\lambda = 1, \quad \gamma_1 = \gamma_2 = 2, \quad Q_p = I_{2\times 2}, \quad R_p = \mathrm{diag}\{0.495, 0.495\}.$$

Also, the activation function $\tanh(e_{u1} + \dot{e}_{u1} - c_i)$ is used for the hidden layer neurons in $F_p(\cdot,\cdot)$, where $\{c_i \,|\, c_1 = -1, c_{i+1} = c_i + 0.05, i = 1, \ldots, 39\}$ are the centres of hidden layer neurons; while $\tanh(e_\lambda + z - c_i)$ with $\{c_i \,|\, c_1 = -30, c_{i+1} = c_i + 0.05, i = 1, \ldots, 119\}$ is used for $F_f(\cdot,\cdot)$.

Additionally, a square wave with amplitude ± 3 and period 1 is used in this simulation for both elements of the injected disturbance ω_l in (1). The desired motion and force trajectories are selected as $u_{1d}(t) = 1.5 + 0.2\cos\pi t$ and $\lambda_d(t) = 60 - 20\cos\pi t$, respectively. The initial conditions are taken to be $u_1(0) = 1.6902, \dot{u}_1(0) = 0$, $z(0) = 0$, and $\lambda(0) = 0$. Also, all the initial weights of the NN devices are taken to be zero.

It is worth looking at the advantages of implanting the learning capacity of NN devices into the nonlinear $H\infty$ control design. For this purpose, the tracking performance of the proposed adaptive $H\infty$ NN controller is compared with that of the controller whose algorithm is exactly the same as the proposed control scheme except that the NN devices are absent. This latter controller represents the underlying suboptimal $H\infty$ only control design in the proposed control scheme and has been discussed in Section V.

Before this performance comparison, it is also of interest to investigate the behaviors of this constrained manipulator under the underlying feedback-linearization-like controller in the proposed control scheme (a similar feedback-linearization based position/force tracking controller using a joint-space reduced-order dynamics was reported in [10]). Since the robustifying terms v_p, v_λ and the NN devices $F_p(\cdot,\cdot), F_f(\cdot,\cdot)$, are all absent, this underlying feedback-linearization-like controller consists of

$$\tau = \begin{bmatrix} \bar{B}_1 \\ \bar{B}_2 - \bar{M}_{21}\bar{M}_{11}^{-1}\bar{B}_1 \end{bmatrix}^{-1} \times \begin{bmatrix} \bar{M}_{11}[\ddot{u}_{1d} - K_v\dot{e}_{u1} - K_p e_{u1}] + \bar{C}_{11}\dot{u}_1 + \bar{G}_1 \\ \Pi^T[\lambda_d + z] + [\bar{C}_{21} - \bar{M}_{21}\bar{M}_{11}^{-1}\bar{C}_{11}]\dot{u}_1 + [\bar{G}_2 - \bar{M}_{21}\bar{M}_{11}^{-1}\bar{G}_1] \end{bmatrix}$$

and

$$\dot{z} = -\mu_z z - \alpha_z e_\lambda$$

with all the parameters being taken to be the same as in the above two controllers. Figs. 3 and 4 show the responses of u_1 and λ of the closed-loop system. It can be seen that this underlying feedback-linearization-like controller cannot make its closed-loop system track the desired force and position trajectories well.

We now present the main simulation results of this section. They are given in Figs. 5–9. Figs. 5 and 6 show the compar-

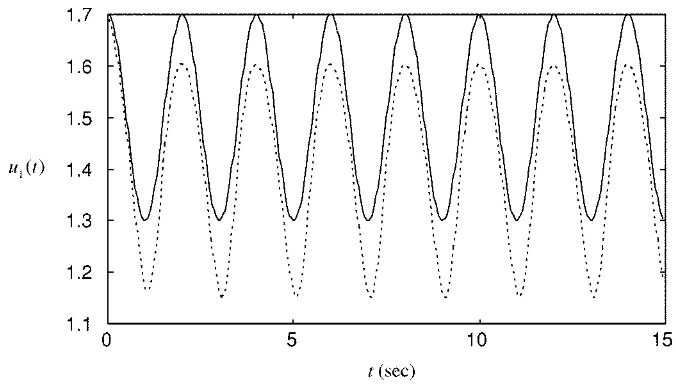

Fig. 3. Response of u_1 of the closed-loop system under the feedback-linearization-like controller (——— : reference u_{1d}; · · · · · · · · · · : feedback-linearization-like controller).

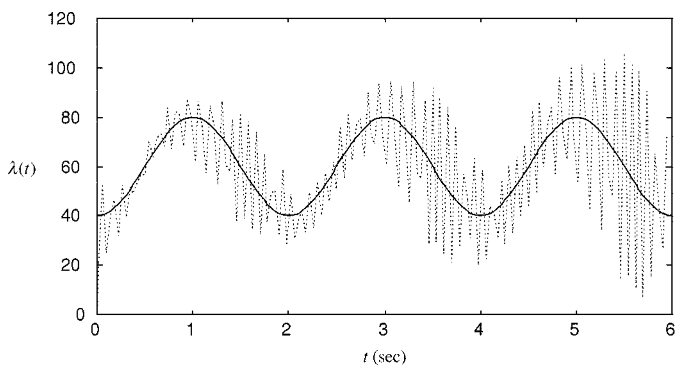

Fig. 4. Response of λ of the closed-loop system under the feedback-linearization-like controller (——— : reference λ_d; · · · · · · · · · · : feedback-linearization-like controller).

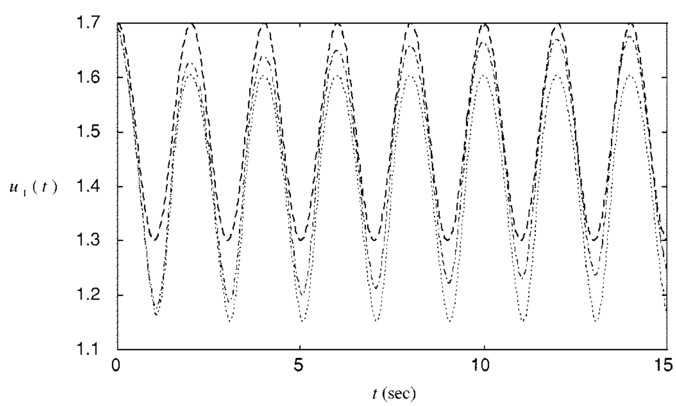

Fig. 5. Motion trajectory $u_1(t)$ (- - - - - - - - - : reference $u_{1d}(t)$; - · - · - · - · - : adaptive $H\infty$ NN controller; · · · · · · · · · · : $H\infty$ only controller).

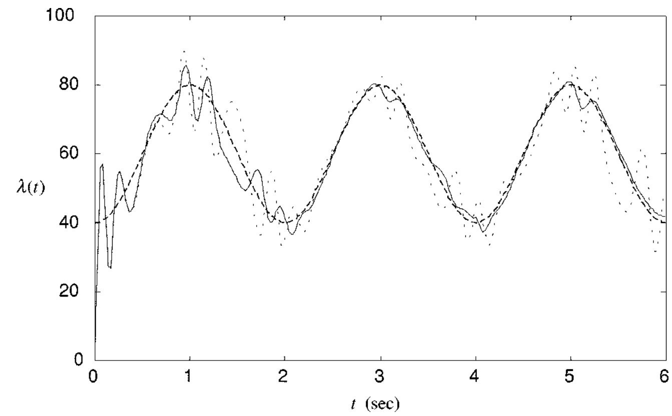

Fig. 6. Force trajectory $\lambda(t)$ (- - - - - - - - - : reference $\lambda_d(t)$; ——— : adaptive $H\infty$ NN controller; · · · · · · · · · : $H\infty$ only controller).

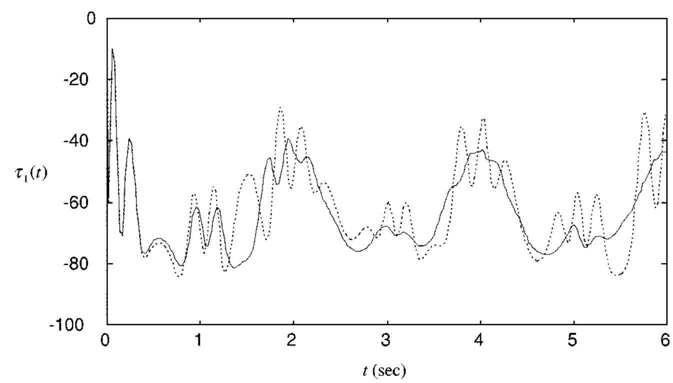

Fig. 7. Applied torque $\tau_1(t)$ (——— : adaptive $H\infty$ NN controller; · · · · · · · · : $H\infty$ only controller).

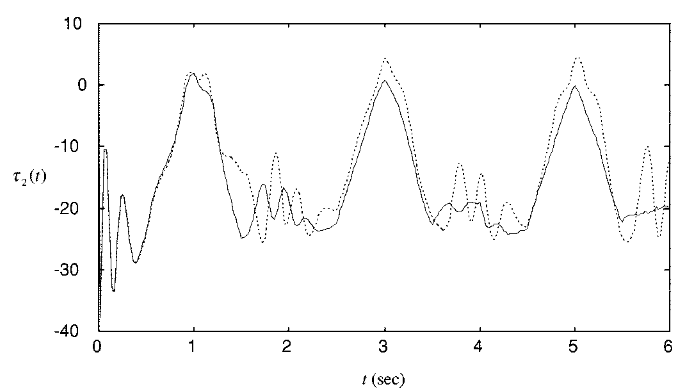

Fig. 8. Applied torque $\tau_2(t)$ (——— : adaptive $H\infty$ NN controller; · · · · · · · · : $H\infty$ only controller).

isons of motion trajectory $u_1(t)$ and force trajectory $\lambda(t)$, respectively. As we can see, the adaptive $H\infty$ NN controller performs better in both force and motion tracking tasks than the suboptimal $H\infty$ only controller. Comparisons of the applied torques τ_1 and τ_2 are depicted in Figs. 7 and 8. It is obvious that, after a period of learning, the amplitudes of both τ_1 and τ_2 used by the adaptive $H\infty$ NN controller are smaller than those of the suboptimal $H\infty$ only controller; also, both τ_1 and τ_2 have fewer oscillations in the closed-loop system controlled by the adaptive $H\infty$ NN controller.

Finally, a comparison of $\int_0^T \{\|x_p\|_{Q_p}^2 + \alpha_\lambda \|e_\lambda\|^2 + (\alpha_\lambda \mu_z/(1+\beta_\lambda))\|z\|^2\}\, dt$, the $H\infty$ tracking performance index, is shown in Fig. 9. From Figs. 7–9, it can be seen that the adaptive $H\infty$ NN position/force tracking controller achieves a better $H\infty$ tracking performance by using preferable torque inputs τ_1 and τ_2. Therefore, it can be concluded that the learning mechanism of NN devices deserves to be implanted into the suboptimal $H\infty$ only control design for the position/force tracking control task of this constrained manipulator.

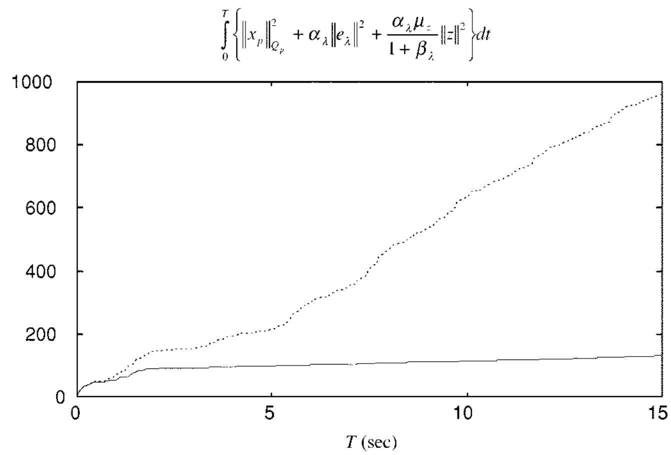

Fig. 9. Response of $\int_0^T \{\|x_P\|_{Q_P}^2 + \alpha_\lambda \|e_\lambda\|^2 + \alpha_\lambda \mu_z / 1 + \beta_\lambda \|z\|^2\}\, dt$(——— : adaptive $H\infty$ NN controller; $\cdots\cdots\cdots$: $H\infty$ only controller).

VII. Conclusion

Using the task-space reduced-order dynamics (11) and the algebraic contact force model (14), it has been shown how both adaptive $H\infty$ NN position/force tracking control and suboptimal $H\infty$ only position/force tracking control can be applied to the simultaneous position/force control problem of constrained manipulators. It is believed that this suboptimal $H\infty$ only position/force tracking control is also new in the robotic control literature. In the adaptive $H\infty$ NN position/force tracking controller, the parametric uncertainties and disturbances in manipulator dynamics as well as the geometry and stiffness uncertainties in environmental modelling are capable of being learned by its NN devices. The effects of the approximation error of NN devices are then attenuated to a prescribed level by the embedded nonlinear $H\infty$ controller. Besides, the NN devices in this controller do not require any time-consuming off-line training phase. Furthermore, this controller can be ultimately less conservative than its counterpart suboptimal $H\infty$ only position/force tracking controller, whenever the adopted NN devices are effective in the sense of Assumption (A6). This was proved in Theorem 3. A simulation study for a constrained two-link planar manipulator was provided. This simulation study showed that the proposed adaptive $H\infty$ NN position/force tracking controller not only can improve the tracking performances of its underlying feedback-linearization-like controller, but also performs better in both force and position tracking tasks than its counterpart suboptimal $H\infty$ only position/force tracking controller.

Acknowledgment

The authors are grateful to the anonymous reviewers for several constructive comments that have improved this paper.

References

[1] B. S. Chen, T. S. Lee, and J. H. Feng, "A nonlinear $H\infty$ control design in robotic systems under parameter perturbation and external disturbance," *Int. J. Contr.*, vol. 59, no. 2, pp. 439–461, 1994.

[2] W. Feng and I. Postletwaite, "Robust non-linear $H\infty$/adaptive control of robot manipulator motion," *Proc. Inst. Mech. Eng. Part I: J. Syst. Contr. Eng.*, vol. 208, no. 14, pp. 221–230, 1994.

[3] P. Tomei, "Nonlinear $H\infty$ disturbance attenuation for robots with flexible joints," *Int. J. Robust Nonlinear Contr.*, vol. 5, pp. 365–373, 1995.

[4] S. Battilotti and L. Lanari, "Adaptive disturbance attenuation with global stability for rigid and elastic joint robots," *Automatica*, vol. 33, pp. 239–243, 1997.

[5] M. T. Grabbe, J. J. Carroll, M. Dawson, and Z. Qu, "Review and unification of reduced-order force control methods," *J. Robot. Syst.*, vol. 10, no. 4, pp. 481–504, 1993.

[6] M. Vukobratovic and A. Tuneski, "Contact control concepts in manipulator robotics—An overview," *IEEE Trans. Ind. Electron.*, vol. 41, pp. 12–24, 1994.

[7] M. Vukobratovic and R. Stojic, "Histroical perspective of hybrid control in robotics: Beginnings, evolution, criticism and trends," *Mech. Mach. Theory*, vol. 30, no. 4, pp. 510–532, 1995.

[8] D. E. Whitney, "Histroical perspective and state of the art in robot force control," *Int. J. Robot. Res.*, vol. 6, no. 1, pp. 3–14, 1987.

[9] M. H. Raibert and J. J. Craig, "Hybrid position/force control of manipulators," *Trans. ASME J. Dyn. Syst. Meas. Contr.*, vol. 103, pp. 126–133, 1981.

[10] N. H. McClamroch and D. Wang, "Feedback stabilization and tracking of constrained robots," *IEEE Trans. Automat. Contr.*, vol. 33, pp. 419–426, 1988.

[11] F. L. Lewis, "Neural network control of robot manipulators," *IEEE Expert*, vol. 11, no. 3, pp. 64–75, 1996.

[12] M. Vukobratovic and D. Katic, "Stabilizing position/force control of robots interacting with environment by learning connectionist structures," *Automatica*, vol. 32, no. 12, pp. 1733–1739, 1996.

[13] S. Jung and T. C. Hsia, "Neural network impedance force control of robot manipulator," *IEEE Trans. Ind. Electron.*, vol. 45, pp. 451–461, 1998.

[14] S. Jung and T. C. Hsia, "Neural network techniques for robust force control of robot manipulators," in *IEEE Int. Symp. Intell. Contr.*, 1995, pp. 111–116.

[15] Y. Zheng, W. Chen, B. You, and H. Cai, "Robotic hybrid position/force control using artificial neural network," in *Proc. SPIE*, vol. 2620, 1995, pp. 603–607.

[16] C. M. Kwan, A. Yesildirek, and F. L. Lewis, "Robust force/motion control of constrained robots using neural network," in *CDC*, vol. 2, 1994, pp. 1862–1867.

[17] M. W. Spong and M. Vidyasagar, *Robot Dynamics and Control*. New York: Wiley, 1989.

[18] K. Hornik, M. Stinchcombe, and H. White, "Multilayer feedforward networks are universal approximators," in *Neural Networks*, 1989, vol. 2, pp. 359–366.

[19] K.-I. Funahashi, "On the approximate realization of continuous mappings by neural networks," in *Neural Networks*, 1989, vol. 2, pp. 183–192.

[20] Y. C. Chang and B. S. Chen, "A nonlinear adaptive $H\infty$ tracking control design in robotic systems via neural networks," *IEEE Trans. Contr. Syst. Technol.*, vol. 5, pp. 13–29, 1997.

[21] D. Hill, R. Ortega, and A. J. van der Schaft, "Nonlinear controller design using passivity and small-gain techniques," presented at the 1994 IEEE CDC Tutorial Workshop, 1994.

[22] M. Vidyasagar, *Nonlinear Systems Analysis*. Englewood Cliffs, NJ: Prentice-Hall, 1993.

[23] L. X. Wang, *Adaptive Fuzzy Systems and Control: Design and Stability Analysis*. Englewood Cliffs, NJ: Prentice-Hall, 1994.

[24] B. S. Chen, C. H. Lee, and Y. C. Chang, "$H\infty$ tracking design of uncertain nonlinear SISO systems: Adaptive fuzzy approach," *IEEE Trans. Fuzzy Syst.*, vol. 4, pp. 32–43, 1996.

Ming-Chang Hwang was born in Taiwan, R.O.C. He received the B.S. degree from National Cheng Kung University, Taiwan, the M.S. degree from National Taiwan University and the M.Eng.St. degree from the University of Queensland, Australia. He is currently pursuing the Ph.D. degree in the School of Electrical and Information Engineering, University of Sydney, Australia. His research interests include robotics, robust control, adaptive control, fuzzy control, neural network control, and system theory.

Xiheng Hu received the M.E. degree from China Agriculture University, the E.E. Diploma and the M.E. degree from Chongqing Architecture Engineering University and Chongqing University, China, respectively, and the Ph.D. degree from the University of Sydney, Australia, in 1991.

He has been a Research Engineer with Mechanical Research Center and a Lecturer at Guazhou Institute of Technology, China. From 1986 to 1991, he was with Eurothem International Australia and BHP International as a Control Application Engineer while pursuing the Ph.D. degree, initially at the University of Wollongong and then the University of Sydney. Since January 1992, he has been with the School of Electrical and Information Engineering, University of Sydney, where he is currently a Senior Lecturer. His present research interests are advanced real time control systems, fuzzy and neural networks, and power control for CDMA communication systems.